Vinpocetine and *Lactobacillus* improve fatty liver in rats: role of adiponectin and gut microbiome

Ahmed M. El-Baz[1]* , Ahmed Shata[2,3], Nehal A. Nouh[4,5], Lubna Jamil[6], Mohamed M. Hafez[7], Sally Negm[8], Attalla F. El-kott[9,10], Mohammed A. AlShehri[9] and Eman M. Khalaf[11]

Abstract

Therapeutics that interfere with the damage/pathogen-associated molecular patterns (DAMPs/PAMPs) have evolved as promising candidates for hepatic inflammation like that occurring in non-alcoholic fatty liver disease (NAFLD). In the current study, we examined the therapeutic impact of the phosphodiesterase-1 inhibitor vinpocetine (Vinpo), alone or when combined with *Lactobacillus*, on hepatic abnormalities caused by a 13-week high-fat diet (HFD) and diabetes in rats. The results show that Vinpo (10 and 20 mg/kg/day) dose-dependently curbed HFD-induced elevation of liver injury parameters in serum (ALT, AST) and tissue histopathology. These effects were concordant with Vinpo's potential to ameliorate HFD-induced fibrosis (Histological fibrosis score, hydroxyproline, TGF-β_1) and oxidative stress (MDA, NOx) alongside restoring the antioxidant-related parameters (GSH, SOD, Nrf-2, HO-1) in the liver. Mechanistically, Vinpo attenuated the hepatocellular release of DAMPs like high mobility group box (HMGB)1 alongside lowering the overactivation of the pattern recognition receptors including, toll-like receptor (TLR)4 and receptor for advanced glycation end-products (RAGE). Consequently, there was less activation of the transcription factor nuclear factor-kappa B that lowered production of the proinflammatory cytokines TNF-α and IL-6 in Vinpo-treated HFD/diabetes rats. Compared to Vinpo treatment alone, *Lactobacillus* probiotics as adjunctive therapy with Vinpo significantly improved the disease-associated inflammation and oxidative stress injury, as well as the insulin resistance and lipid profile abnormalities via enhancing the restoration of the symbiotic microbiota. In conclusion, combining Vinpo and *Lactobacillus* probiotics may be a successful approach for limiting NAFLD in humans.

Keywords Vinpocetine, Probiotics, NAFLD, Phosphodiesterase-1, DAMPs, Gut microbiome

*Correspondence:
Ahmed M. El-Baz
Elbaz_pharmacy@yahoo.com; ahmed.elbaz@deltauniv.edu.eg
[1]Department of Microbiology and Immunology, Faculty of Pharmacy, Delta University for Science and Technology, Gamasa 11152, Egypt
[2]Department of Clinical Pharmacology, Faculty of Medicine, Mansoura University, Mansoura 35516, Egypt
[3]Department of Clinical Pharmacology, Faculty of Medicine, Horus University-Egypt, New Damietta 34518, Egypt
[4]Department of Microbiology, Medicine Program, Batterjee Medical College, P.O. Box 6231, Jeddah 21442, Saudi Arabia
[5]Inpatient Pharmacy, Mansoura University Hospital, Mansoura 35516, Egypt

[6]Department of Histology, Faculty of Medicine, October 6 University (O6U), 6th of October City, Egypt
[7]Biochemistry Department, Faculty of Pharmacy, Ahram Canadian University, 6th of October City, Egypt
[8]Department of Life Sciences, College of Science and Art Mahyel Aseer, King Khalid University, Abha 62529, Saudi Arabia
[9]Department of Biology, College of Science, King Khalid University, Abha 61421, Saudi Arabia
[10]Department of Zoology, Faculty of Science, Damanhour University, Damanhour 22511, Egypt
[11]Department of Microbiology and Immunology, Faculty of Pharmacy, Damanhour University, Damanhour 22511, Egypt

Introduction

Non-alcoholic fatty liver disease (NAFLD) involves an abnormal fat deposition in the liver hepatocytes (>5%) of patients who are not ingesting alcohol. This metabolic hepatic disorder has a high prevalence percentage ranging from 25 to 30% in adults (Younossi et al. 2018). The pathogenic sequence of NAFLD starts with simple fatty liver (steatosis) and may transfer to steatohepatitis (NASH), followed by fibrosis, cirrhosis (Lonardo et al. 2018) and hepatocellular carcinoma (HCC) (Younossi et al. 2018). Insulin resistance makes the liver susceptible to other factors that trigger hepatocellular damage. Hyperinsulinemia elicits a rise in hepatic de novo lipogenesis alongside adipose tissue lipolysis that synergistically drives higher transfer of free fatty acids toward the hepatocytes of the liver (Postic and Girard 2008). Oxidative damage, adipokines dysregulation, inflammatory mediators, and hepatic stellate cell activation are involved in promoting NAFLD progression (Yilmaz 2012).

The ester of vincamine known as vinpocetine (Vinpo) is extracted from the periwinkle plant. Vinpo has a cerebroprotective impact that can ameliorate brain disorders, including memory disturbances, cognitive impairment, stroke, and dementia (Zhao et al. 2011). Besides possessing a high safety profile, no substantial toxicity for Vinpo has been reported on long-term use so far (Zhang et al. 2018). Vinpo causes vasodilation by inhibiting the cyclic nucleotide phosphodiesterase-1 (PDE-1), voltage-gated sodium channels, and calcium channels, and raising oxygen and glucose consumption in the brain. Besides, Vinpo has antioxidant, anti-inflammatory, and anti-thrombotic effects (Essam et al. 2019).

The gut-liver axis (GLA) is a bidirectional functional relationship that exists between the gastrointestinal tract and the liver. Changes in one component, like the gut microbiota or gut barrier, will affect the liver condition due to the close functional and anatomical association (Mazzotti et al. 2016). Dysbiosis of the gut microbiota and the intestinal epithelial barrier has also been attributed to various diseases, including fatty liver. A former study showed that the intestinal microbiota of NAFLD patients has a lower diversity than those of healthy individuals (Saltzman et al. 2018). Previous studies reported the increase in abundance of *Proteobacteria, Lachnospiraceae Enterobacteriaceae* including *Escherichia*, and *Bacteroidetes*, in the overall population of fatty liver patients, while several studies find a reduction or no difference in *Bacteroidetes*, as well as a drop in *Prevotella* and *Firmicutes* (Gómez-Zorita et al. 2019). Otherwise, the gut microbiota can directly affect the body weight that can worsen the NAFLD (Jayakumar and Loomba 2019). Accordingly, it seems reasonable to find that probiotics can improve the health of the host by their capability to restore the normal symbiotic status of the gut microbiota and treat digestive issues when consumed in an adequate amount (El-Baz et al. 2020).

FDA-approved treatments for NAFLD are still lacking, and the precise mechanisms underlying the disease's progression remain unclear. Considering this, we examined the underlying mechanism of Vinpo in treating fatty liver disease in this experimental animal model study and clarified the function of *Lactobacillus* probiotics as an adjuvant therapy by assessing the relative abundance of specific gut microbiota members linked to fatty liver disease.

Materials and methods

Chemicals and reagents

Vinpo was supplied as 5 mg of Vinporal tablet (Amyria Co., Egypt) and prepared as 0.5% w/v suspension in carboxymethyl cellulose (CMC). *Lactobacillus* was purchased in the form of Lacteal forte sachets (Rameda Pharma Co, Giza, Egypt). The sachet contained 1×10^{10} microbial cells of *Lactobacillus delbrueckii* and *Lactobacillus fermentum* (Garcia-Castillo et al. 2019). The components of the sachet were dispersed in water and each rat was ingested 0.5 ml of microbial suspension containing 2.7×10^8 CFU/ml (Fooladi et al. 2015). Streptozotocin (STZ), CMC, cholesterol, and cholic acid were provided from Sigma Chemical Co. (St. Louis, Missouri, USA).

Animals and experimental design

Male adult Sprague Dawley rats (180–220 g) were accustomed to the environment for a week before the experiment began. Rats were housed under typical nutritional and environmental conditions for the duration of the experiment. The experimental protocol was approved by the Delta University, Faculty of Pharmacy's research ethics committee (ethical approval number: FPDU11/2022). A high-fat diet (HFD) containing 10% sugar, 10% lard stearin, 2% cholesterol, and 0.5% cholic acid was administered for 13 weeks to rats. Rats were given an intraperitoneal injection of STZ (30 mg/kg in citrate buffer, 1 ml/kg) after four weeks. The levels of fasting blood glucose (FBG) were assessed seven days after STZ injection. Only diabetic rats—those with FBG readings exceeding 200 mg/dL—were allowed to complete the test. The HFD was left unaltered after STZ treatment, but sugar was taken out to prevent excessive hyperglycemia (El-Derany and El-Demerdash 2020). With the beginning of the 6th week of the HFD, the 8-week treatment phase of the study continued till the end.

The study layout consisted of 7 groups ($n=6$–8): the first three groups were fed a normal chow diet and either given no treatment (Normal), oral 20 mg/kg of Vinpo suspended in CMC (Vinpo) or *Lactobacillus* as mentioned earlier (Lacto). The other four groups were fed with HFD and were administered either no treatment (HFD), oral

El-Baz *et al. AMB Express*   (2024) 14:89

Page 3 of 16

10 mg/kg of Vinpo (Vinpo 10+HFD), 20 mg/kg of Vinpo (Vinpo 20+HFD), or 20 mg/kg of Vinpo and *Lactobacillus* (Vinpo 20/Lacto+HFD).

Oral vinpocetine 20 mg/kg (Petric et al. 2023; Zhang et al. 2018) suspended in CMC (Vinpo) or *Lactobacillus* (El-Baz et al. 2023) as mentioned earlier (Lacto). The other four groups were fed HFD and either administered no treatment (HFD), vinporal 10 mg/kg (Vinpo 10+HFD), Vinporal 20 mg/kg (Vinpo 20+HFD) or vinporal 20 mg/kg and *Lactobacillus* (Vinpo 20/Lacto+HFD).

Animal sacrifice and sample collection

Following the experiment, rats were starved overnight. The following day, they were weighed and injected with thiopental to make them comatose. After blood samples were drawn via cardiac puncture and centrifuged at 3000 rpm for 20 min, the serum was separated and preserved at − 80 °C for analysis. Additionally, the livers of every animal were taken out, cleaned, weighed, and washed in ice-cold phosphate-buffered saline (PBS, pH 7.4). The liver tissues were divided into pieces and mashed (10% w/v) in 20 mM Tris-HCl (pH 7.4) with 1 mM EDTA and then centrifuged at 3000 g for 20 min at 4 °C. For upcoming biochemical studies, the supernatants were collected and kept at − 80 °C. Liver sections were preserved in 10% neutral buffered formalin solutions for histological examination. Moreover, 300 mg cecal faeces samples were weighed shortly after the animals were put down to collect stool samples. DNA was extracted using the QIAamp DNA Stool Mini Kit (Qiagen Inc., cat. # 51504 Hilden, Germany) in accordance with the manufacturer's recommendations. The acquired DNA was kept at − 20 °C and subjected to spectrophotometric analysis using a NanoDrop device (Jenway Nano, UK) to determine the DNA concentration. The remaining faeces samples were kept at − 80 °C until they were needed once more.

Biochemical assessments for liver injury and lipid in serum samples

The injury of the liver was assessed biochemically by estimating serum concentrations of alanine transaminase (ALT), aspartate transaminase (AST), and alkaline phosphatase (ALP) by the commercially available kits (Spectrum Diagnostics, Cairo, Egypt). Triglycerides (TGs), total cholesterol (TC), and high-density lipoprotein cholesterol (HDL-C) serum concentrations were determined following the methods reported by Fossati and Prencipe (1982), Allain et al. (1974) and Lopes-Virella et al. (1977), respectively, utilizing kits purchased from Biodiagnostics (Cairo, Egypt).

Histopathological and immunohistochemical assessments of the liver samples

Samples of excised hepatic tissue were fixed in neutral buffered formalin (10%). Using customary histological techniques, the tissue was treated, and paraffin blocks were made. Necroinflammation and fibrosis changes were evaluated using the Ishak-modified HAI method in sections (5 μm thick) stained with hematoxylin-eosin and Mallory's trichrome, respectively (Ishak et al. 1995). The following NAFLD activity scores (NAS) were used to assess the severity of hepatic steatosis, inflammation, and ballooning. Grades 0–3 for hepatocellular steatosis were assigned to the specimens: grade 0, where less than 5% of the hepatic parenchyma was affected by steatosis; grade 1, where 6–33% of the hepatic parenchyma were affected; grade 2, where 34–66% of the hepatic parenchyma were affected; and grade 3 when steatosis occupied more than 66% of the hepatic parenchyma). For hepatic ballooning, the specimens were divided into classes 0–2 (grade 0, no ballooning; grade 1, little balloon cells; and grade 2, numerous cells/notable ballooning). According to the amount of inflammatory cell infiltration, the specimens were grouped into classes 0–3 (grade 0, no infiltration; grade 1, 1–2 foci every 400× field; grade 2, 3–4 foci every 400× field; and grade 3, more than 4 foci every 400× field). Hepatic fibrosis was classified into stages 0–4 (stage 0: no fibrosis; stages 1 and 2: mild to moderate periportal and perisinusoidal fibrosis; stage 3: bridging fibrosis; and stage 4: cirrhosis).

Concerning liver immunohistochemical assessment, for the purpose of identifying target proteins, 5 μm paraffin-embedded sections were placed on coated glass slides, and endogenous peroxidases and non-specific protein binding were blocked. Slide sections were first treated with primary antibodies, followed by HRP-conjugated secondary antibodies and substrate/chromogen for color development. Nuclear factor-kappa B (NF-κB), TLR4, HMGB-1 and RAGE (Santa Cruz Biotechnology, CA, USA) are the primary antibodies utilized in this investigation. The ImageJ software (NIH, Bethesda, MD, USA) was used to perform quantifications of the immunohistochemical results.

Hepatic hydroxyproline determination

To determine how much collagen was deposited in the liver, the hydroxyproline content was measured as previously explained (Bergman and Loxley 1963). Briefly stated, a section of the liver was submerged in KOH (5%) for a whole night at 37 °C, hydrolyzed with NaOH (10 N), and then incubated with Chloramine-T for three hours at 25 °C. Ehrlich's reagent was then added to the reaction mixture and heated to 60 °C for 20 min. The resulting color's spectrophotometric absorbance at 550 nm was measured.

El-Baz *et al. AMB Express*   (2024) 14:89

Page 4 of 16

Enzyme-linked immunosorbent assay (ELISA)

Using ELISA kits, tissue lysates were used for the determination of TNF-α (RayBiotech Inc., Norcross, GA, USA), TGF-β1 (eBioscience, Vienna, Austria), Nrf-2 and HO-1 (Cloud-Clone Co., Houston, USA). On the other hand, adiponectin (Assaypro, St. Louis, MO, USA) and leptin (RayBiotech Inc., Norcross, GA, USA) were determined in serum. To make tissue lysates, 35 mg of tissue was minced in 0.315 ml of ice-cold lysis buffer (10 mM Tris pH 7.4, 150 mM NaCl, 0.5% v/v Triton X-100), which also contained a protease inhibitor. The supernatants were then separated by centrifugation at 5000×*g* for 10 min at 4 °C. Eventually, 96-well plates were filled with tissue lysate supernatants for ELISA.

Assessment of oxidative stress and antioxidant parameters in the liver

Portions of liver samples (10% w/v) were minced in an ice-cold buffer (20 mM Tris-HCl, 1 mM EDTA, pH 7.4) by a Potter-Elvehjem homogenizer, followed by centrifugation at 3000×*g* for 20 min at 4 °C to collect supernatants.

Hepatic malondialdehyde content determination

The concentration of malondialdehyde (MDA) was calculated as previously mentioned (Gérard-Monnier et al. 1998). In a nutshell, 0.3 ml of liver homogenate sample was added to 0.65 ml of 10.3 mM 1-methyl-2-phenylindole in acetonitrile mixed with methanol containing 32 mM $FeCl_3$ (3:1) and vortexed. The samples were thoroughly mixed, sealed with a tight stopper, and incubated at 45 °C for 60 min after the addition of 0.15 ml of 37% (v/v) HCl. After being chilled on ice, the samples were centrifuged at 4000×*g* for 10 min, and the absorbance at 586 nm was determined spectrophotometrically. For the quantification of MDA, a standard curve made of 1,1,3,3-tetramethoxypropane was also used.

Hepatic nitric oxide content determination

According to a prior description (Miranda et al. 2001), the total nitrate/nitrite (NOx) products were calculated as a measure of nitric oxide (NO^-) synthesis. 0.25 ml of 0.3 N NaOH was mixed with 0.5 ml of liver homogenate. For deproteinization, 0.25 ml of 5% (w/v) $ZnSO4$ was added after the mixture had been incubated for 5 min at room temperature. After centrifuging this mixture at 3000×*g* for 20 min at 4 °C, 0.4 ml of the supernatant was added to 0.3 ml of Vanadium chloride (8 mg/ml) in 1 M HCl and 0.3 ml of Griess reagent [0.15 ml of 2% (w/v) sulfanilamide in 5% (v/v) HCl and 0.15 ml of 0.1% (w/v) N-(1-naphthyl)-ethylendiamine dihydrochloride in distilled water]. Spectrophotometric measurements of the samples were made at 540 nm after 45 min of incubation at 37ºC. $NaNO_3$ (0–100 nmol/ml) was used to construct a standard curve for determination of NOx concentration in samples.

Hepatic reduced glutathione content determination

With a small alteration, hepatic reduced glutathione (GSH) was measured as stated previously (Moron et al. 1979). Summarily, 0.45 ml of liver homogenate was centrifuged at 1000×*g* for 5 min after the protein was precipitated with 0.05 ml of 50% (w/v) trichloroacetic acid. After 5 min at room temperature, the reaction mixture of 0.25 ml of supernatant, 1 ml of 0.2 M Tris-HCl (including 1 mM EDTA, pH 8.9), and 0.05 ml of 10 mM 5,50-dithio-bis-(2-nitrobenzoic acid) in absolute methanol was measured spectrophotometrically at 412 nm. The calculations were done using a standard GSH curve (0–500 nmol/ml).

Hepatic superoxide dismutase activity determination

Superoxide dismutase (SOD) activity was assessed in a manner slightly different from that described earlier (Marklund and Marklund 1974). This technique is based on SOD's capacity to prevent pyrogallol's autoxidation. Briefly, 1.5 ml of 20 mM Tris-HCl (including 1 mM EDTA, pH 8.2) and 0.1 ml of 15 mM pyrogallol were combined with 0.1 ml of liver homogenate. After that, the increase in OD for the samples at 420 nm was observed for 3 min in order to calculate the change in OD per minute. By running a control under the same circumstances without any sample, the percentage of inhibition for the samples was calculated. One unit of SOD enzyme activity was defined as the amount of the enzyme that reduced the rate of pyrogallol autoxidation by 50%.

Real-time PCR test for measuring relative abundance of some selected gut microbiota

The relative abundances of *Bifidobacteria* spp., *Lactobacillus spp., Bacteroides*, *Escherichia coli*, *Clostridium* spp., *Fusobacteria* spp., *Porphyromonas gingivalis*, *Providencia* spp., and *Prevotella intermedia* were assessed by the quantitative real-time polymerase chain reaction (RT-PCR) technique. By utilizing adequate primers for 16 S rRNA housekeeping gene amplification, the total number of bacteria was calculated (Table S1). For quantitation of DNA, 40–80 ng of isolated fecal DNA was combined with 12.5 µl (2×) SYBR Green PCR master mix (Willowfort Co., Birmingham, UK.) and 1.5 µl of each forward and reverse primer (10 µM each). A final volume of 25 µl was created by adding 7.5 µl of nuclease-free water. In a RT-PCR system (QuantStudio, ThermoFisher Scientific, USA), RT protocol was started at 95 °C for 5 min, then 45 cycles of 95 °C for 20 s, annealing for 20 s (Table S1), followed by 40 s at 72 °C and 5 min at 72 °C as the final extension (Wong et al. 2017).

Statistical analysis

Values in each experimental group were presented as a mean±SE. The one-way analysis of variance test ensued by Tukey's multiple comparison test was used to analyze parametric data. For non-parametric data, the Kruskal–Wallis test and Dunn's multiple comparison test were used. Statistical analyses were carried out by GraphPad Instat V 3.1 (GraphPad Inc., San Diego, CA, USA) with a cut-off level of statistical significance<0.05.

Results

Vinpo and its combination with *Lactobacillus* ameliorated HFD-induced liver injury

The liver enzymes AST, ALT, and ALP significantly increased in rats fed HFD alone. Treatment with Vinpo prevented these parameters from rising. The addition of *Lactobacillus* improved the liver damage markers even further (Fig. 1A–C). However, there were no discernible differences in albumin levels between the groups (Fig. 1D). When liver sections from the group exposed to HFD/STZ were examined histopathologically, they revealed congested blood vessels, occluded sinusoids, diffuse hydropic degeneration with macro-vesicular steatosis. Portal fibrosis appears in some sections infiltrated

with leukocytes. Vinpo therapy resulted in a dose-dependent milder pathological alteration. Histopathological alterations were further restored with the inclusion of *Lactobacillus* (Fig. 2A; Table S2).

Vinpo and its combination with *Lactobacillus* resolved liver fibrosis in HFD/STZ induced NASH

The collagen accumulation was assessed histologically and biochemically in the liver. Histological analysis of Mallory's trichrome stained liver sections showed excess bluish stained collagen deposition around central vein and portal areas in rats exposed to HFD/STZ. On the other hand, collagen deposition was prevented by Vinpo therapy, whether it was administered alone or in conjunction with *Lactobacillus* (Fig. 2B; Table S2). Biochemically, liver hydroxyproline level was greatly increased in rats when subjected to HFD and STZ compared to the control group. Rats co-treated with vinpocetine significantly decreased hydroxyproline level (Fig. 3A). Furthermore, rats exposed to HFD showed a significant elevation in hepatic TGF-β1 as compared to the control group. Treatment of rats with Vinpo induced a significant reduction in serum level of TGF-β1 as compared to non-treated rats (Fig. 3B). *Lactobacillus* addition significantly
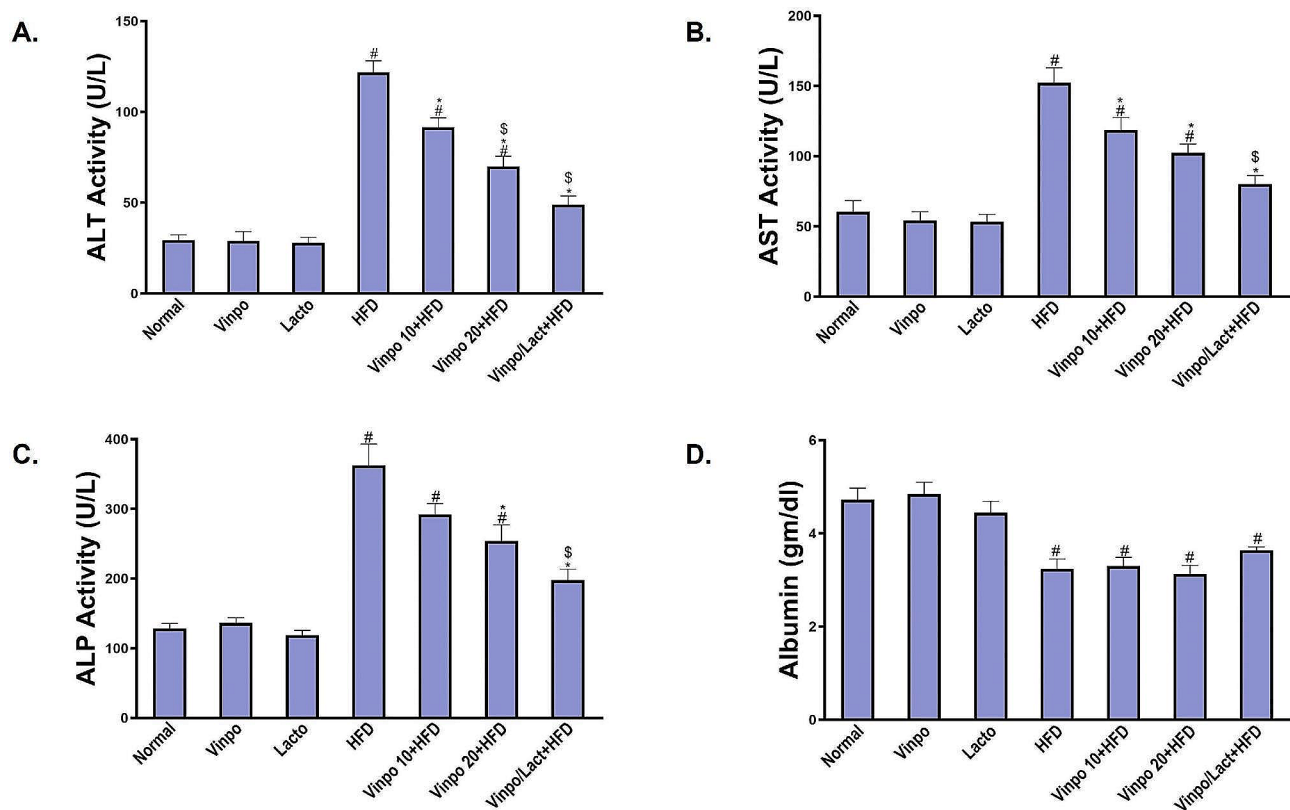
Fig. 1 Effect of vinpocetine (Vinpo 10 and 20 mg/kg) and *Lactobacillus* (Lacto) treatments on HFD-induced changes in serum aspartate transaminase (ALT, **A**), alanine transaminase (AST, **B**), alkaline phosphatase (ALP, **C**) and albumin (**D**). Bars are means±SE (*n*=6–8 per group). Statistical significances are presented as: # vs. Normal group; * vs. HFD group and § vs. Vinpo 10+HFD

El-Baz *et al. AMB Express*   (2024) 14:89

Page 6 of 16
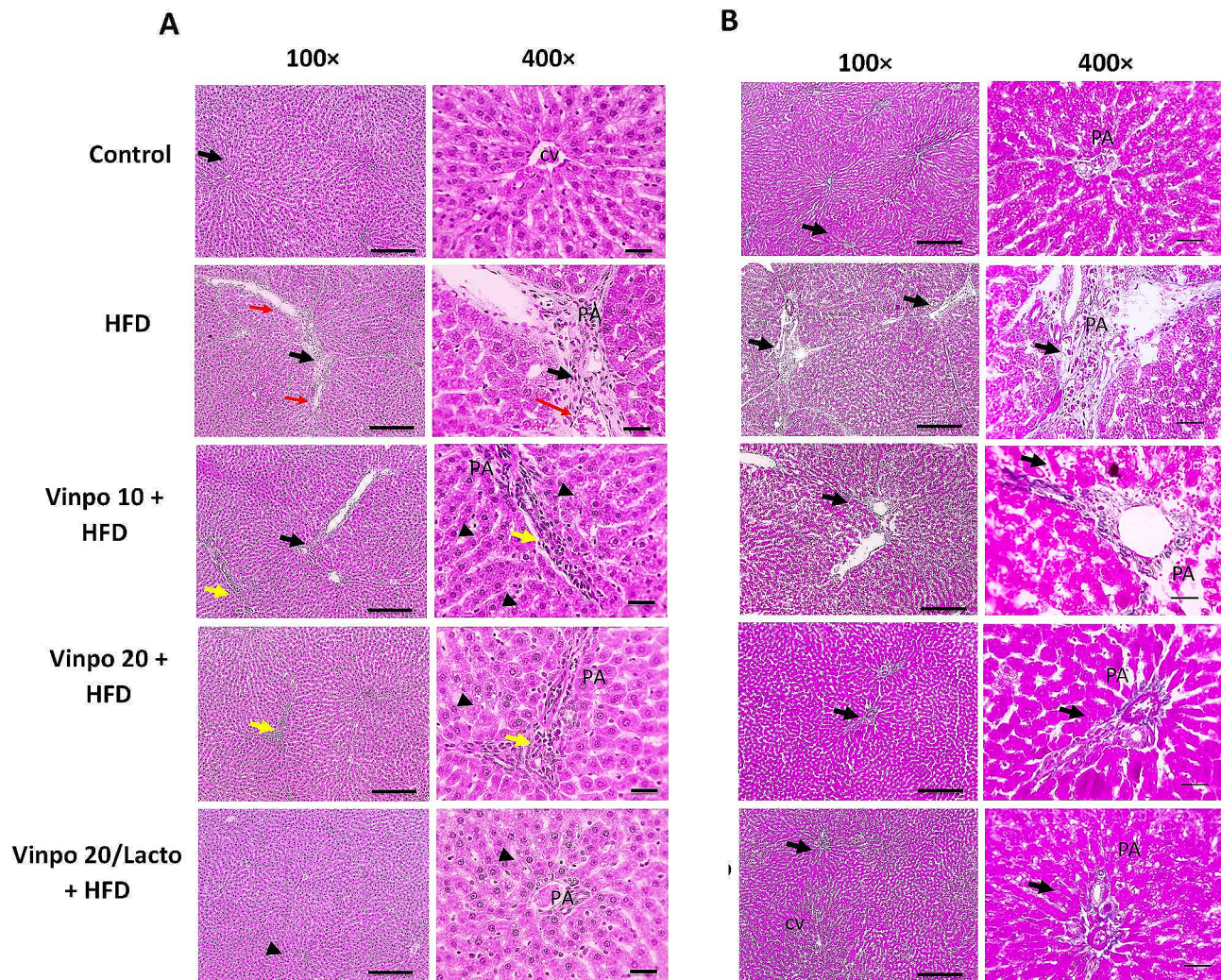
Fig. 2 Effect of vinpocetine (Vinpo 10 and 20 mg/kg) and *Lactobacillus* (Lacto) treatments on HFD-induced changes in liver histopathology. Representative pictures of hematoxylin-eosin (**A**) and Mallory's trichrome (**B**) stainings (Low magnification 100×; bar 100 µM, high magnification 400×; bar 50 µM) showing normal hepatocytes arranged in radiating plates around central vein (CV) with normal portal areas (PA) and sinusoids in normal group. **A** liver sections from HFD group showing congested blood vessels (red arrow), occluded sinusoids, diffuse hydropic degeneration with macro-vesicular steatosis (arrowheads). Portal fibrosis appears in some sections infiltrated with leukocytes (black arrows). Liver sections showing milder pathological changes in the treated groups including: few micro-vesicular steatosis (arrowheads), mild portal fibrosis (thin black arrow) and inflammation (yellow arrow) in Vinpo10+HFD group, few micro-vesicular steatosis (arrowheads), mild portal inflammation (yellow arrow) in Vinpo20+HFD group, very few micro-vesicular steatosis (arrowheads) in Vinpo20/Lacto+HFD group. **B** Normal liver sections showed no collagen deposition around CV or PA. Meanwhile, liver sections from HFD group showing excess bluish stained collagen deposition around CV or PA (black arrows). Liver sections from the treated groups showing decreased bluish stained collagen deposition around CV or PA (black arrows) in Vinpo10+HFD group, much less bluish stained collagen deposition around CV or PA (black arrows) in Vinpo20+HFD group, no excess bluish stained collagen deposition around CV or PA in Vinpo20/Lacto+HFD group

increases the inhibitory impact of Vinpo on TGF-β1 and hydroxyproline when compared to Vinpo treated groups alone.

Vinpo and its combination with *Lactobacillus* reverses HFD-induced lipid panel alterations

Comparing the NASH group to the normal group, there was a discernible rise in cholesterol and TG levels as well as a fall in HDL serum levels (Fig. 4A-C). The cholesterol levels in HFD-groups treated by Vinpo 10 or 20 mg/kg groups were lesser than those of the HFD/STZ group.

When *Lactobacillus* is added, the inhibitory action is significantly increased. However, only simultaneous administration of Vinpo and *Lactobacillus* effectively reduced TG. None of the therapeutic groups' HDL levels have differed noticeably from those of the NASH group.

Vinpo and its combination with *Lactobacillus* restored HFD induced adiponectin and leptin alterations

To obtain insight into the protective mechanisms of Vinpo against hepatic steatosis in HFD-fed rats, we measured the levels of adiponectin and leptin to determine
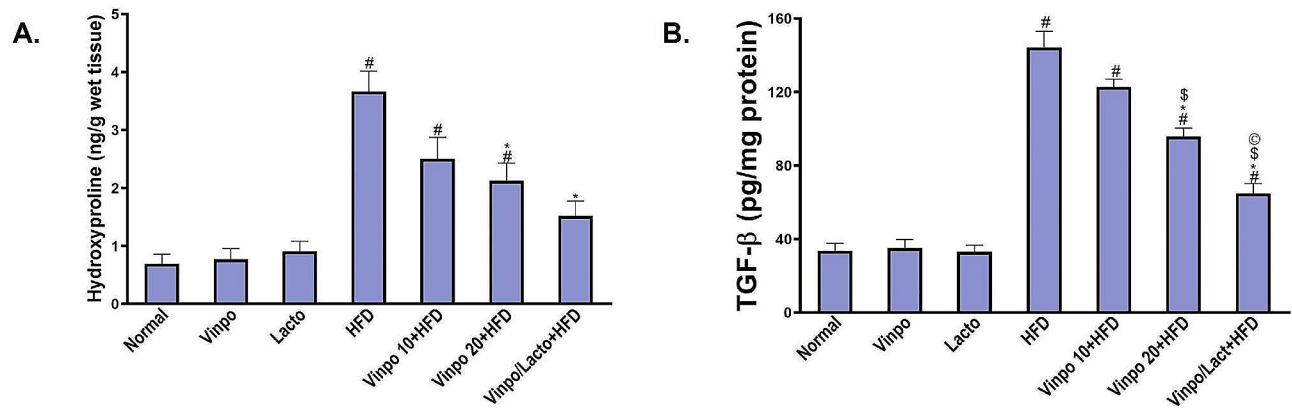
Fig. 3 Effect of vinpocetine (Vinpo 10 and 20 mg/kg) and *Lactobacillus* (Lacto) treatments on HFD-induced changes in hepatic tissue hydroxyproline (**A**) and TGF-β_1 (**B**). Bars are means ± SE (*n* = 6–8 per group). Statistical significances are presented as: # vs. Normal group; * vs. HFD group; § vs. Vinpo 10 + HFD and © vs. Vinpo 20 + HFD
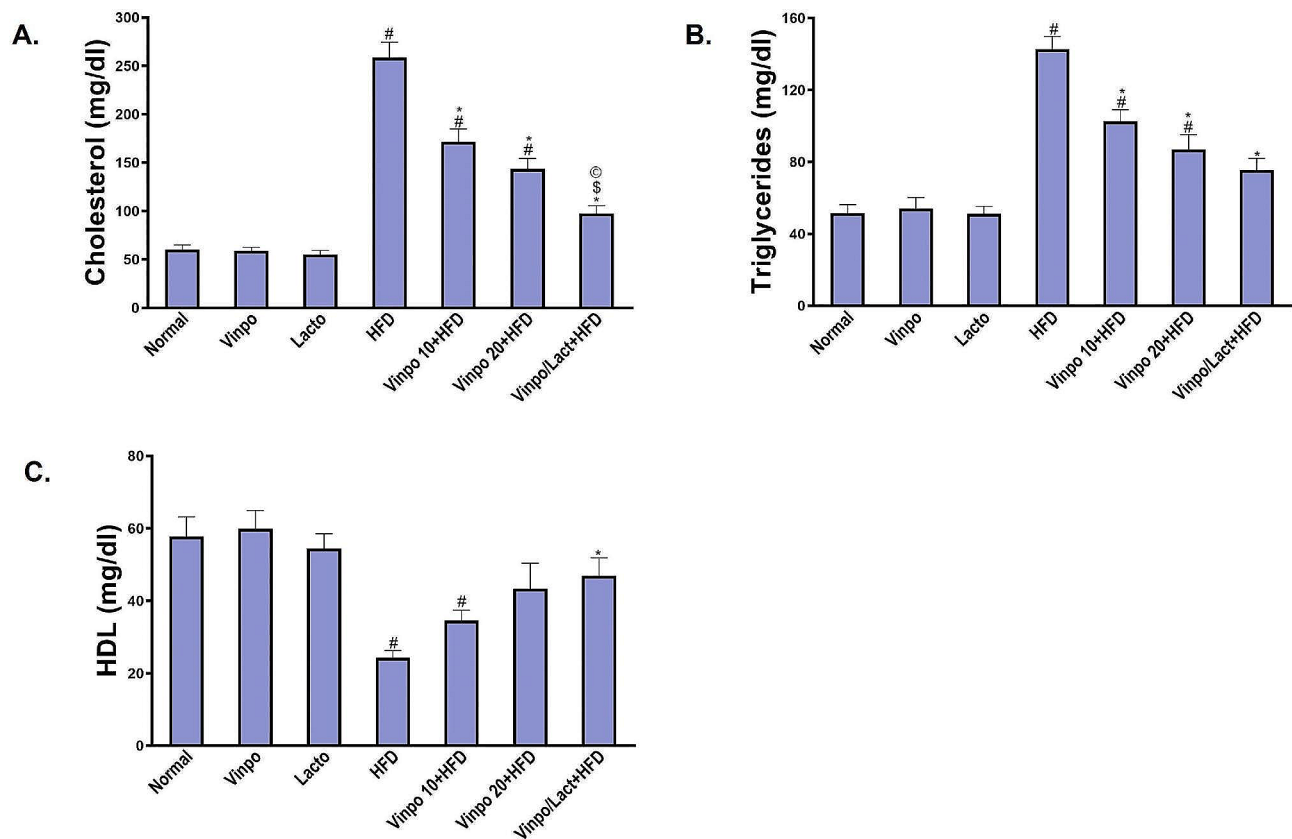
Fig. 4 Effect of vinpocetine (Vinpo 10 and 20 mg/kg) and *Lactobacillus* (Lacto) treatments on HFD-induced changes in serum cholesterol (**A**), triglycerides (TG, **B**) and high-density lipoprotein (HDL, **C**). Bars are means ± SE (*n* = 6–8 per group). Statistical significances are presented as: # vs. Normal group; * vs. HFD group; § vs. Vinpo 10 + HFD and © vs. Vinpo 20 + HFD

whether improvement in insulin resistance is a factor in the positive effect of Vinpo and *Lactobacillus*. When compared to the control group, the HFD group's levels of leptin dramatically increased while Adiponectin greatly reduced (Fig. 5A and B). It's interesting that Vinpo, especially at a dose of 20 mg, reversed these abnormalities brought on by HFD. These markers further improved when *Lactobacillus* and Vinpo 20 mg were given simultaneously.

Vinpo and its combination with *Lactobacillus* ameliorated HFD-induced oxidative stress and Nrf2/HO-1 expression

Next, we examined whether the protective effects of Vinpo and *Lactobacillus* against HFD/STZ-induced fatty
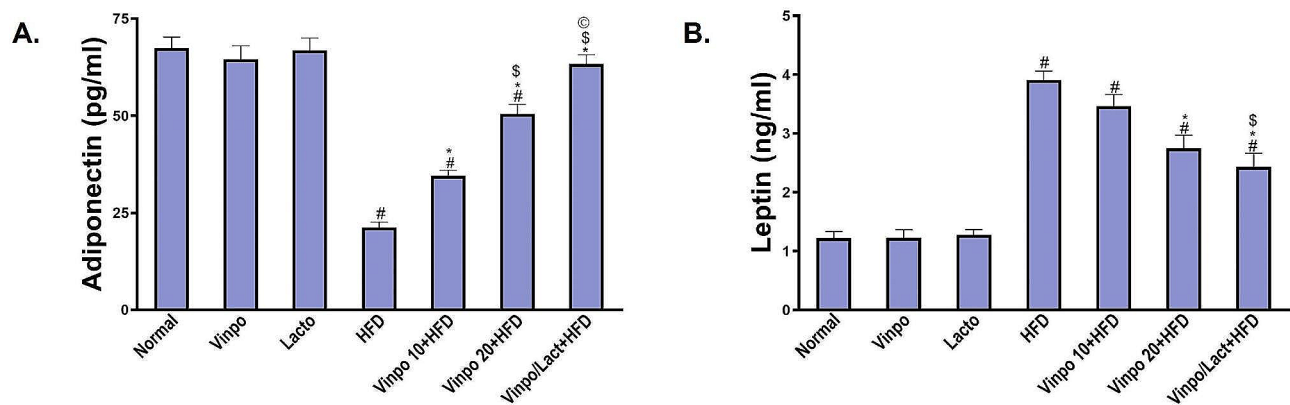
Fig. 5 Effect of vinpocetine (Vinpo 10 and 20 mg/kg) and *Lactobacillus* (Lacto) treatments on HFD-induced changes in serum adiponectine (**A**) and leptin (**B**). Bars are means ± SE (*n* = 6–8 per group). Statistical significances are presented as: # vs. Normal group; * vs. HFD group; § vs. Vinpo 10 + HFD and © vs. Vinpo 20 + HFD

liver involve reducing oxidative stress. As seen in Fig. 6 A–D, untreated HFD-rat livers experienced a considerable hepatic increase in MDA and nitrite, as well as NOx alongside a significant decrease in SOD and GSH, when compared to the normal counterparts. All treated groups demonstrated a statistically significant decline in MDA and restoration in GSH, compared to HFD-group. Furthermore, compared to the 10 mg/kg dose, the 20 mg/kg of Vinpo considerably reduces MDA. Only Vinpo 20 mg/kg treatment group and its combination with *Lactobacillus* showed a significant improvement in SOD compared to the HFD group. The addition of *Lactobacillus* to Vinpo had a significant effect on MDA and SOD as compared to the Vinpo alone treated group. Next, we evaluated the expression of Nrf-2 and HO-1 which confer cytoprotection against oxidative stress-induced cellular damage. The HFD group dramatically decreased HO-1 and NrF2 compared to the control group. In contrast to the HFD group, significant improvements in NrF2 and HO-1 were observed in the group treated with Vinpo 20 and to a greater extent when combined with *Lactobacillus* (Fig. 6E and F).

Vinpo and its combination with *Lactobacillus* ameliorated HFD-induced inflammation

It was observed that hepatic inflammation was successfully induced by giving rats HFD and a single STZ injection. This was demonstrated by the significant increase in liver concentrations of the inflammatory cytokines TNF-α and IL-6 in HFD-untreated rats. However, Vinpo administration was able to reverse the inflammation that HFD had caused, as shown by the significantly reduced tissue levels of TNF-α and IL-6 when compared to the HFD group. When *Lactobacillus* was added to Vinpo, these effects were more prominent (Fig. 7A and B). We then investigated the potential mechanism that could be responsible for these elevated inflammatory cytokines.

HMGB1, TLR-4, RAGE, and NF-κB immunohistochemistry evaluations were then performed to identify whether Vinpo protective effects involve a lessening of the release of DAMPs and activation of PRRs. While tissue hepatic sections from the NASH untreated HFD-group were shown to have more brown color than the controls, Vinpo treatment, especially at a dose of 20 mg/kg, significantly reduced the hepatic overexpression of HMGB1, TLR-4, RAGE, and NF-κB, as shown by the significant decrease in brown staining compared to in HFD-rat livers (Figs. 8 and 9, respectively). Co-administration of *Lactobacillus* further decreased brown staining indicating its additional protective impact.
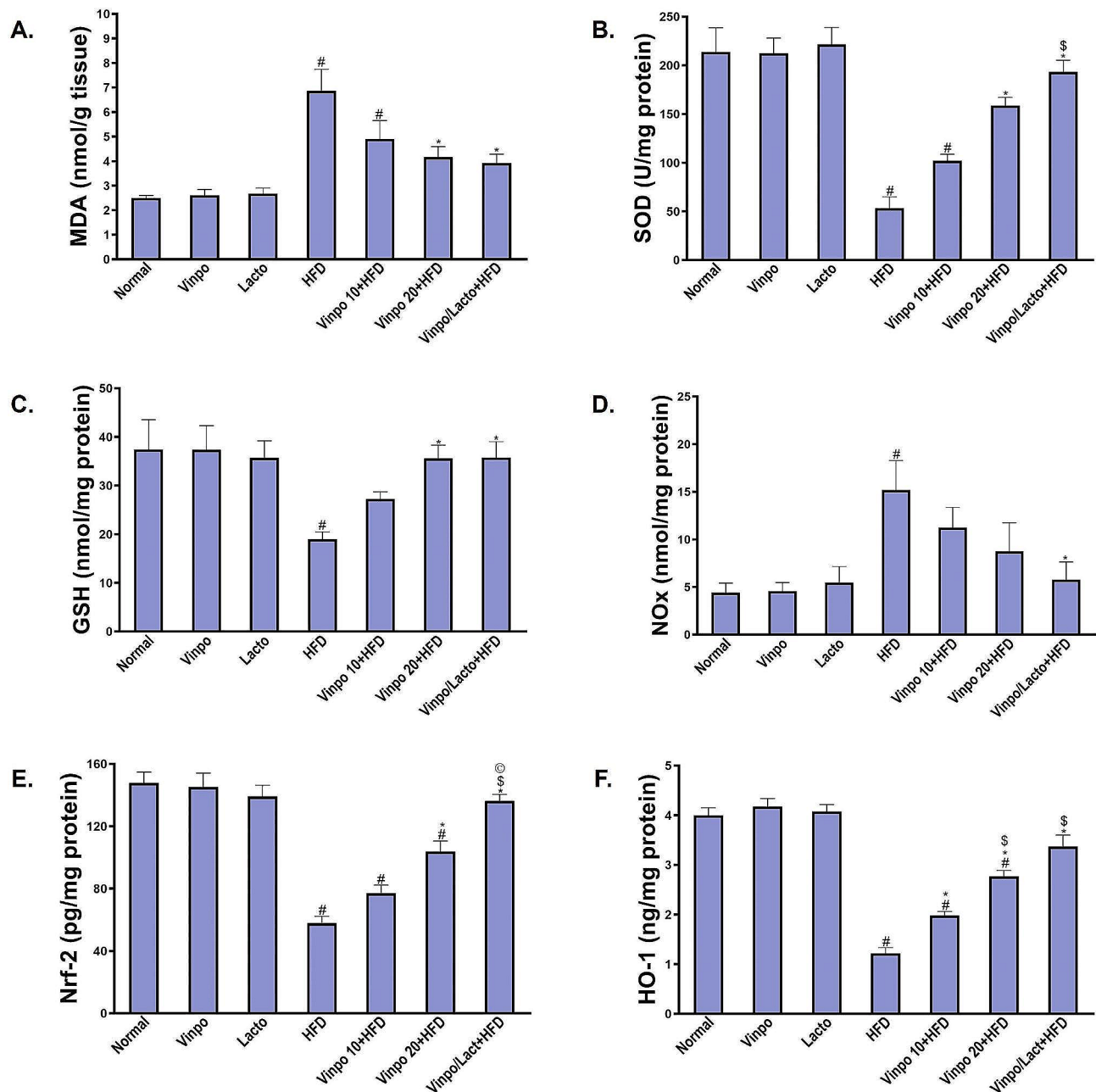
Effect of Vinpo and *Lactobacillus* combination on gut microbiota composition

Across the examined groups in the current investigation, a change in gut microbiota composition was observed. A remarkable variation of the relative abundance of intestinal microbial flora, with NAFLD being associated with a significant decline in *Bifidobacteria* spp. and *Lactobacillus* spp. as compared to healthy controls. *Bacteroides* spp., *Fusobacterium* spp., *E. coli*, *Clostridium* spp., *Providencia* spp., *Prevotella intermedia*, and *Porphyromonas gingivalis* were significantly abundant compared to the normal healthy control group. In the current investigation, when compared to the positive control group, the administration of combination therapy of Vinpo and *Lactobacillus* probiotics significantly enhanced the restoration of the symbiotic gut microbiota (Fig. 10).

Discussion

Current NAFLD management therapies are primarily focused on dietary and lifestyle changes, with discrepancies in the clinical results due to low patient compliance. So far, no pharmaceutical therapy or surgical methods have been approved for the treatment of
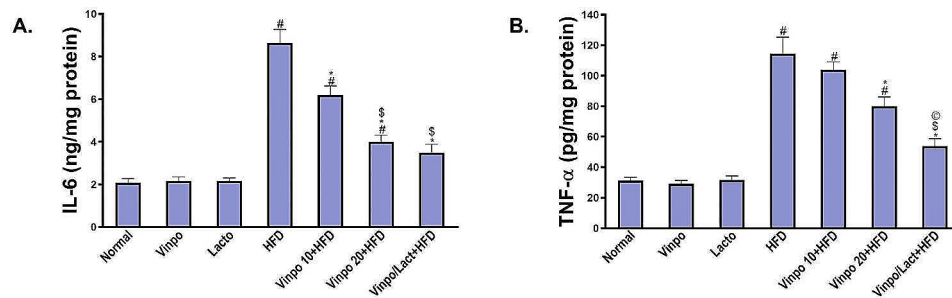
Fig. 6 Effect of vinpocetine (Vinpo 10 and 20 mg/kg) and *Lactobacillus* (Lacto) treatments on HFD-induced changes in hepatic tissue malondialdehyde (MDA, **A**); superoxide dismutase (SOD, **B**); reduced glutathione (GSH, **C**); total nitrate/nitrite (NOx, **D**), Nrf-2 (**E**) and HO-1 (**F**). Bars are means ± SE (*n* = 6–8 per group). Statistical significances are presented as: # vs. Normal group; * vs. HFD group; § vs. Vinpo 10 + HFD and © vs. Vinpo 20 + HFD

NAFLD. Meanwhile, hypolipidemic medicines, anti-TNF, antioxidants, and diabetic medications are merely recommended for attenuating the progress of NAFLD (Mantovani and Dalbeni 2021). Dysregulation of the gut microbiome, or dysbiosis, is among the factors implicated in driving different pathways that aggravate the steatosis and inflammation cascades in the liver of NAFLD patients (Campo et al. 2019). Otherwise, the activation of the cAMP/PKA or cGMP-dependent signaling pathways in the liver can impair lipogenesis and glycogenesis

via multiple mechanisms (Wahlang et al. 2018). Phosphodiesterase (PDE) inhibitors can be sustained in both pathways, which may be useful in the setting of fatty liver disease. Accordingly, we investigated whether the PDE-1 inhibitor Vinpo would ameliorate the HFD-induced steatosis and inflammation in rat livers, and if so, Vinpo would exhibit better efficacy when combined with *Lactobacillus*.

Vinpo significantly lowered the HFD-induced rise in serum ALT, AST, and ALP activities and improved the
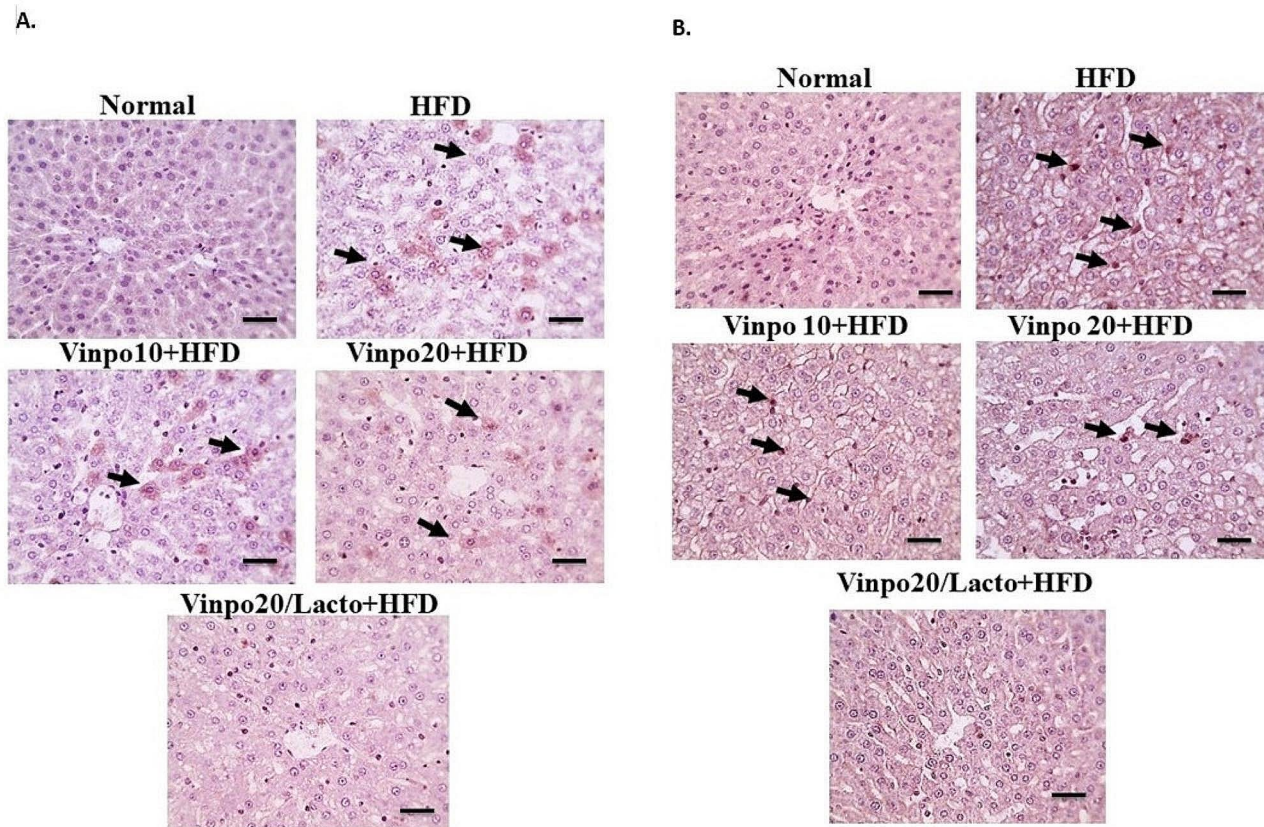
Fig. 7 Effect of vinpocetine (Vinpo 10 and 20 mg/kg) and *Lactobacillus* (Lacto) treatments on HFD-induced changes in hepatic tissue IL-6 (**A**) and TNF-α (**B**). Bars are means ± SE (n = 6–8 per group). Statistical significances are presented as: # vs. Normal group; * vs. HFD group; § vs. Vinpo 10 + HFD and © vs. Vinpo 20 + HFD
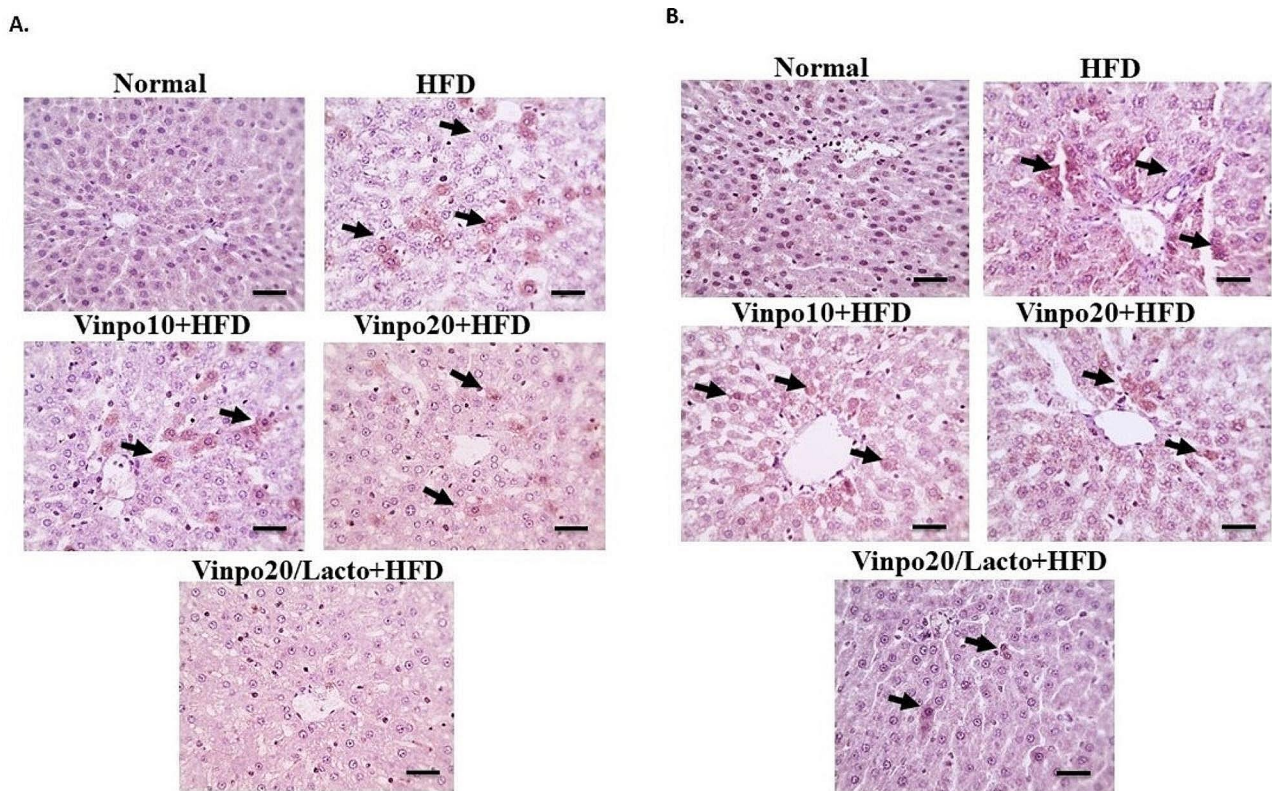
Fig. 8 A Effect of vinpocetine (Vinpo 10 and 20 mg/kg) and *Lactobacillus* (Lacto) treatments on HFD-induced changes in hepatic high mobility group box 1 (HMGB1) protein immunostaining (×400) showing negative staining in normal group. Meanwhile, liver sections from HFD group showing significant positive brown cytoplasmic staining of many hepatocytes (black arrows). Liver sections from the treated groups showing decreased positive brown cytoplasmic staining that appears in some hepatocytes (black arrows) in Vinpo10 + HFD group, much less positive cytoplasmic staining that appears in few hepatocytes (black arrows) in Vinpo20 + HFD group, very mild positive brown cytoplasmic staining of very few hepatocytes (black arrows) in Vinpo20/Lacto + HFD group. IHC counterstained with Mayer's hematoxylin. **B** Effect of vinpocetine (Vinpo 10 and 20 mg/kg) and *Lactobacillus* (Lacto) treatments on HFD-induced changes in hepatic toll like receptor-4 (TLR-4) immunostaining (400×) showing negative staining in normal group. Meanwhile, liver sections from HFD group showing significant positive brown cytoplasmic staining in many hepatocytes (black arrows). Liver sections from the treated groups showing decreased positive brown cytoplasmic staining that appears in some hepatocytes (black arrows) in Vinpo10 + HFD group, much less positive cytoplasmic staining that appears in few hepatocytes (black arrows) in Vinpo20 + HFD group, very mild positive brown cytoplasmic staining that appears in very few hepatocytes (black arrows) in Vinpo20/Lacto + HFD group. IHC counterstained with Mayer's hematoxylin

hepatic architecture of steatotic rats, especially at a dose of 20 mg/kg. On the lipid profile, Vinpo caused a mediocre decrease in the elevation caused by HFD in serum total cholesterol, but not TGs and HDL. Moreover, the HFD-induced decline of adiponectin and escalation of leptin were reversed by Vinpo at doses of 10 and, more pronouncedly, 20 mg/kg. Both adiponectin's increase and leptin's decrease mediated by Vinpo are reliable evidence for improving the insulin sensitivity and lipid metabolism in HFD rats (Forny-Germano et al. 2018). Interestingly,

Fig. 9 **A** Effect of vinpocetine (Vinpo 10 and 20 mg/kg) and *Lactobacillus* (Lacto) treatments on HFD-induced changes in hepatic receptors for advanced glycation end products (RAGEs) immunostaining (400×) showing negative staining in normal group. Meanwhile, liver sections from HFD group showing significant positive brown cytoplasmic staining of many hepatocytes (black arrows). Liver sections from the treated groups showing decreased positive brown cytoplasmic staining that appears in some hepatocytes (black arrows) in Vinpo10 + HFD group, much less positive cytoplasmic staining that appears in few hepatocytes (black arrows) in Vinpo20 + HFD group, very mild positive brown cytoplasmic staining of very few hepatocytes (black arrows) in Vinpo20/Lacto + HFD group. IHC counterstained with Mayer's hematoxylin. **B** Effect of vinpocetine (Vinpo 10 and 20 mg/kg) and *Lactobacillus* (Lacto) treatments on HFD-induced changes in hepatic nuclear factor-kappa B (NF-κB) immunostaining (400×) showing negative staining in normal group. Meanwhile, liver sections from HFD group showing prominent positive brown nuclear staining of many von kupffer cells (black arrows). Liver sections from the treated groups showing decreased positive brown nuclear staining that appears in some von kupffer cells (black arrows) in Vinpo10 + HFD group, much less positive brown nuclear staining that appears in few von kupffer cells (black arrows) in Vinpo20 + HFD group, negative staining of von kupffer cells in Vinpo20/Lacto + HFD group. IHC counterstained with Mayer's hematoxylin

concomitant administration of *Lactobacillus* with Vinpo (20 mg/kg) exhibited the maximal efficacy in restoring these abnormalities elicited by HFD to an extent near the normal control group.

The anticipated manifestations of the fatty liver disease were evident in the rats by a marked rise in the indexes of inflammation (TNF-α and IL-6) and fibrosis (TGF-β1 and hydroxyproline). Meanwhile, these abnormalities were countered by treating the rats with Vinpo (20 mg/kg) alone and, more pronouncedly, when combined with *Lactobacillus*. The inflammation in fatty liver disease arises from the excessive generation of DAMPs "Damage-associated molecular patterns" from the dying hepatocytes. HMGB1 is a key DAMP and driver for the sterile inflammatory response upon release from necrotic hepatocytes. HMGB1 mediates chemoattraction of the inflammatory cells to the liver through stimulating TLR4 localized on Kupffer cells and other hepatic immune cells recruited in the setting of HFD-induced NAFLD in mice (Li et al. 2011; Shaker 2022). Besides TLR4, HMGB1 can stimulate the receptors for advanced glycation end products (RAGEs), which are expressed on hepatic DCs, neutrophils, monocytes, and, to a lesser extent, on Kupffer cells (Sims et al. 2010; Zhong et al. 2020). Stimulation of both TLR4 and RAGE localized on hepatic immune cells by HMGB-1 or lipopolysaccharides (LPS) will subsequently activate diverse downstream pathways like mitogen-activated protein kinases (MAPKs), NF-κB, interferon regulatory factor 1 (IRF1) and NADPH oxidase (Guimaraes et al. 2010; Yan et al. 2023; Zeng et al. 2004). Eventually, this will produce exuberant inflammatory mediators and ROS that aggravate the initial insult and amplify the hepatic inflammation.
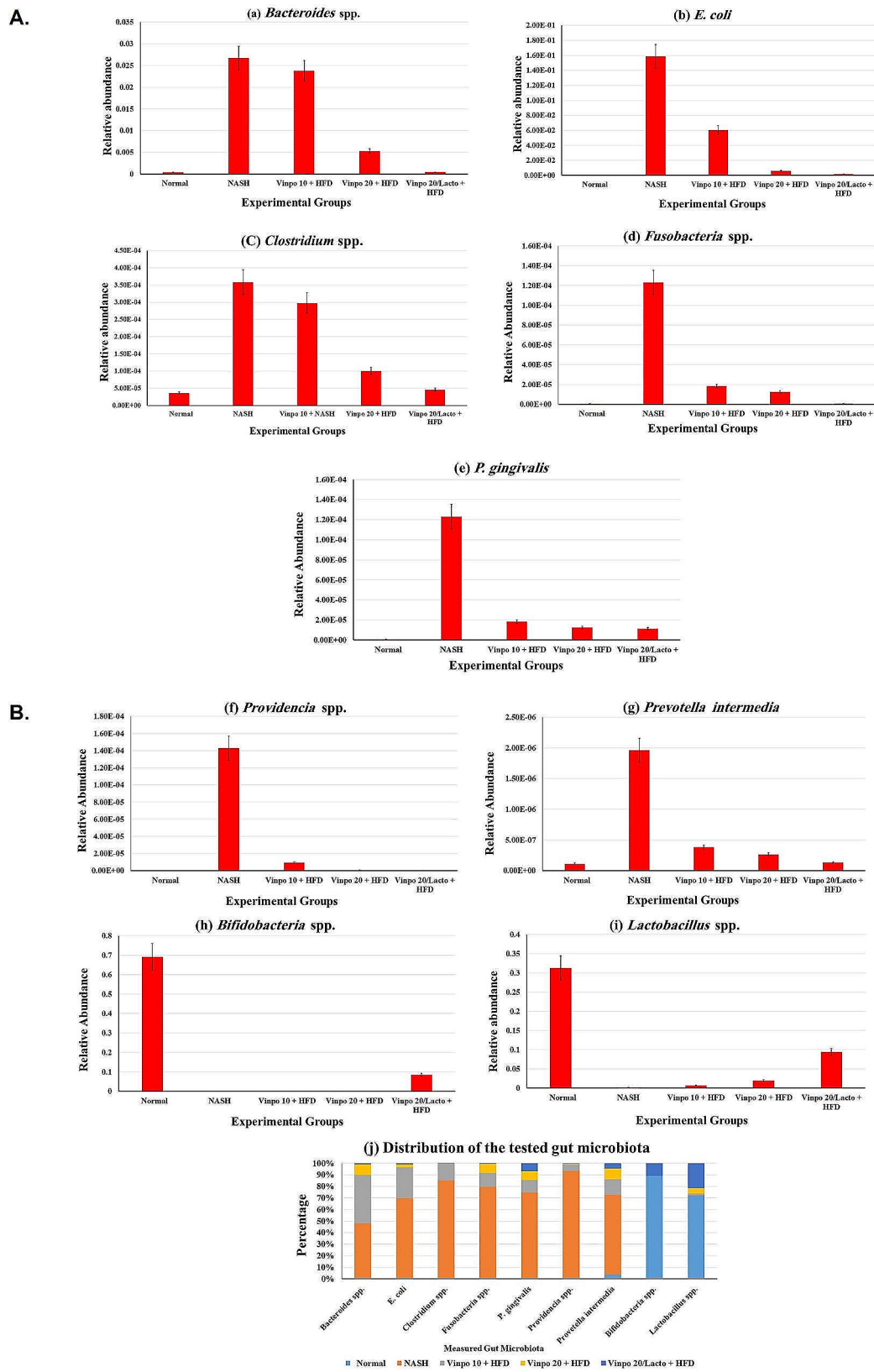
Fig. 10 Relative abundance (RA) of different microbial species in different groups of tested samples in the fatty liver animal model. RA is calculated for different groups of tested samples through targeted genes specific to different reference microbiota relative to the control housekeeping 16 S rRNA gene. **a** *Bacteroides* spp., **b** *E. coli*, **c** *Clostridium* spp., **d** *Fusobacteria* spp, **e** *P. gingivalis*., **f** *Providencia* spp., **g** *Prevotella intermedia*, **h** *Bifidobacteria* spp., **i** *Lactobacillus* spp., and **j** Distribution of the tested gut microbiota

Vinpo (20 mg/kg) alone or with *Lactobacillus* successfully lowered the higher nuclear translocation of the transcription factor NF-κB in the hepatic cells of the HFD-rats. Besides TLR4, NF-κB is translocated to the nucleus after stimulation of pattern recognition receptors like TLR9, IL-1R, and TNF-R. For instance, TLR9 senses the denatured DNA released from host dying hepatocytes and upregulates the inflammatory cytokines like IL-1β and TNF-α *via* activating the transcription factor NF-κB (Bamboat et al. 2010). Thus, the hepatocellular protection of the Vinpo and *Lactobacillus* combination will also decrease the release of HMGB1 and other DAMPs like the denatured DNA, leading to less activation of the NF-κB and upregulation of the proinflammatory cytokines.

The beneficial effects of Vinpo against the hepatocellular damage instigated by HFD were also mediated by countering the oxidative stress as evidenced by limiting the rise of the lipid peroxidation product MDA and the nitrite products in the liver. These data were concordant with the impact of Vinpo in restoring the HFD-induced depletion of the hepatic non-enzymatic antioxidant GSH and enzymatic antioxidant SOD. Activation and transcription of Nrf2 have a key role in HO-1 expression to protect hepatocytes from injury caused by oxidative stress alongside inducing antioxidant enzymes like SOD and GSH-peroxidase (Solano-Urrusquieta et al. 2020). Besides, Nrf2 negatively regulates genes that foster hepatic steatosis (Chambel et al. 2015; Galicia-Moreno et al. 2020). Based on these, Vinpo direct inducing effect on Nrf2 accounts for reversing the HFD-induced decrease of the hepatic content of HO-1 alongside those of GSH and SOD. Similarly, *Lactobacillus* promoted the beneficial impact of Vinpo on oxidative stress and antioxidant parameters.

Based on previous literature, NAFLD strongly correlates to the gut microbiome (Castillo et al. 2021; Lee et al. 2021). Our study investigated the NAFLD-associated gut microbial signatures and the augmentative role of *Lactobacillus* probiotics in enhancing the therapeutic effect of Vinpo. *Lactobacilli*, *Bifidobacteria*, and *Streptococci* can be naturally found in some foods, and are commonly used as commercial probiotics that control the abundance of gut gram-negative bacteria and are strongly involved in research trials for the treatment of NAFLD and NASH (Koopman et al. 2019). Our study recorded *Lactobacillus* spp. and *Bifidobacterium* spp. as health indicator gut taxa that significantly declined in abundance in the induced-fatty liver group. Their normal healthy levels were restored upon treatment with Vinpo. Simultaneously, *Bacteroides* spp., *E. coli*, *Clostridium* spp., *Fusobacteria* spp. *P. gingivalis*, *Prevotella intermedia*, and *Providencia* spp. were enriched in the induced-disease group and identified as proinflammatory gut microbiota members in NAFLD.

Previous studies demonstrated the richness of *Fusobacterium* and *Escherichia* in patients with NAFLD (Su et al. 2024). *Fusobacteria* phylum and *Fusobacteriaceae* family were previously reported for their increased abundance in NAFLD patients compared to healthy individuals, probably due to their implication in triggering the inflammatory signaling during the disease progression (Kim et al. 2019; Li et al. 2011; Shen et al. 2017). Our study reported a high abundance of *Fusobacteria* spp. among the NAFLD group compared to healthy and treated groups especially those receiving the combination of *Lactobacillus* and Vinpo. In general, *E. coli* is consistently identified as a disease indicator taxon associated with type-2 diabetes mellitus and NAFLD (El-Baz et al. 2021; Khalaf et al. 2022; Wang et al. 2016). Our findings were in line with the previously published work where the NASH group showed a significant increase in *E. coli* abundance that has been reduced in a dose-dependent pattern upon treatment with Vinpo. Interestingly, the coadministration of *Lactobacillus* spp. probiotics significantly diminished the proliferation of *E. coli*, restoring its level in healthy groups.

Moreover, the literature reported a reduction in *Bacteroides fragilis* abundance (Gómez-Zorita et al. 2019), nevertheless, in this study, *Bacteroides* spp. increased in abundance aligning with the published discrepancies regarding the taxon proliferation according to the measured species and the applied treatment (Fig. 10). Oxidative balance is crucial for mitochondrial function and regulates the metabolic pathways of antioxidants, especially glutathione. A decrease in intracellular glutathione can lead to oxidative stress (Mardinoglu et al. 2015). During dysbiosis, the microbiota consumes glycine, a glutathione precursor, leading to a deficiency in glutathione production and consequently, oxidative stress. *Clostridium sensu stricto* is notably abundant in mice with NASH. Treatment with glycine-based tripeptide DT-109 replenishes glutathione, reducing *C. sensu stricto* abundance, lipogenesis, and lipotoxicity while enhancing fatty acid oxidation (Rom et al. 2020). A previous study demonstrated that *Lactobacillus rhamnosus* GG (LGG) boosts the intracellular antioxidant pool and activates the Nrf2 antioxidant signaling pathway, preventing liver injury from acetaminophen and ethanol toxicity (Saeedi et al. 2020). These findings align with our study, which showed an increased abundance of *Clostridium* spp. that was reversed upon treatment with Vinpo and *Lactobacillus* probiotic combination.

In our study, *Prevotella intermedia* significantly increased in the NAFLD group compared to the healthy one, however, its proliferation was significantly reduced upon treatment with Vinpo at different concentrations

El-Baz *et al. AMB Express*   (2024) 14:89

Page 14 of 16

where the highest level of significance was recorded upon the coadministration of *Lactobacillus* probiotics. Interestingly, *P. gingivalis,* a common oral pathogen worldwide was recently reported to be implicated in the development of NAFLD because of the contribution of the pathogen LPS to the activation of NF-κB and JNK signaling pathways (Ding et al. 2019). Furthermore, recent studies have identified *P. gingivalis* as a direct risk factor for NAFLD due to its disruption of metabolic and immunologic regulatory pathways (Liu et al. 2023). According to our study, the increased abundance of *P. gingivalis* was associated with the NAFLD group that significantly decreased by Vinpo alongside *Lactobacillus* spp. *Providencia rettgeri* was reported as one of the intestinal microbiota members that contributes to choline metabolism into trimethylamine and subsequently, trimethylamine N-oxide that reduces hepatic cholesterol and improves the blood lipid profile (Bluemel et al. 2016; Li et al. 2021). However, the abnormally increased choline metabolism could lead to liver steatosis due to reduced choline levels (Bluemel et al. 2016). This explains the association of increased abundance of *Providencia* spp. in our study with NAFLD diseased group that significantly reversed upon treatment with Vinpo.

The findings of this study align with the reported therapeutic effects of both *Lactobacillus fermentum* (*Limosilactobacillus fermentum* CQPC06) and *Lactobacillus delbrueckii* probiotics in the treatment of NAFLD, where *Lactobacillus fermentum* mitigated lipid metabolism issues and fat accumulation by regulating the expression of various proteins and genes and contributed to reducing ROS levels in the liver, as well as *Lactobacillus delbrueckii* improved the liver histology and reduced steatohepatitis (Mijangos-Trejo et al. 2023).

In conclusion, Vinpo dose-dependently mitigated the hepatic injury, steatosis, and inflammation elicited by HFD in rats. Our findings helped us understand the mechanisms behind the beneficial effects of Vinpo including insulin sensitivity improvement, attenuation of oxidative stress, and dampening of the sterile inflammatory response. Importantly, the reported microbial gut signatures in this study open the horizon for developing novel diagnostic lab testing for the early diagnosis of NAFLD and highlighting the importance of the concomitant administration of *Lactobacillus* spp. probiotics with Vinpo for augmented therapeutic action.

Abbreviations

HFD	High-fat diet
NAFLD	Non-alcoholic fatty liver disease
DAMPs	Damage-associated molecular patterns
PAMPs	Pathogen-associated molecular patterns
ALT	Alanine transaminase
AST	Aspartate transaminase
HMGB	High mobility group box
TLRs	Toll-like receptors
NASH	Non-alcoholic steatohepatitis
SOD	Superoxide dismutase
GSH	Glutathione
TNF-α	Tumor necrosis factor alpha
MDA	Malondialdehyde
Nrf2	Nuclear factor erythroid 2
HO-1	Heme oxygenase-1
TGF-β_1	Transforming growth factor beta
NF-kB	Nuclear factor kappa B
IL-6	Interleukin 6
GLA	Gut-liver axis
PDE-1	Phosphodiesterase-1

Supplementary Information

The online version contains supplementary material available at https://doi.org/10.1186/s13568-024-01731-2.

Supplementary Material 1

Data availability
Enquiries about data availability should be directed to the authors.

Declarations

Conflict of interest
The authors declare no competing interests.

Ethical approval
The experimental protocol was permitted by Research Ethics Committee, Faculty of Pharmacy, Delta University for Science and Technology (ethical approval number: FPDU11/2022).

Consent for publication
Not applicable.

References
Allain CC, Poon LS, Chan CS, Richmond W, Fu PC (1974) Enzymatic determination of total serum cholesterol. Clin Chem 20(4):470–475

Bamboat ZM, Balachandran VP, Ocuin LM, Obaid H, Plitas G, DeMatteo RP (2010) Toll-like receptor 9 inhibition confers protection from liver ischemia-reperfusion injury. Hepatology 51(2):621–632. https://doi.org/10.1002/hep.23365

Bergman I, Loxley R (1963) Two improved and simplified methods for the spectrophotometric determination of hydroxyproline. Anal Chem 35(12):1961–1965. https://doi.org/10.1021/ac60205a053

Bluemel S, Williams B, Knight R, Schnabl B (2016) Precision medicine in alcoholic and nonalcoholic fatty liver disease via modulating the gut microbiota. Am J Physiol Gastrointest Liver Physiol 311(6):G1018–g1036. https://doi.org/10.1152/ajpgi.00245.2016

Campo L, Eiseler S, Apfel T, Pyrsopoulos N (2019) Fatty liver disease and gut microbiota: a comprehensive update. J Clin Transl Hepatol 7(1):56–60. https://doi.org/10.14218/jcth.2018.00008

Castillo V, Figueroa F, González-Pizarro K, Jopia P, Ibacache-Quiroga C (2021) Probiotics and prebiotics as a strategy for non-alcoholic fatty liver disease, a narrative review. Foods https://doi.org/10.3390/foods10081719

Chambel SS, Santos-Goncalves A, Duarte TL (2015) The dual role of Nrf2 in non-alcoholic fatty liver disease: regulation of antioxidant defenses and hepatic lipid metabolism. Biomed Res Int https://doi.org/10.1155/2015/597134

Ding LY, Liang LZ, Zhao YX, Yang YN, Liu F, Ding QR, Luo LJ (2019) Porphyromonas gingivalis-derived lipopolysaccharide causes excessive hepatic lipid accumulation via activating NF-κB and JNK signaling pathways. Oral Dis 25(7):1789–1797. https://doi.org/10.1111/odi.13153

El-Baz AM, Khodir AE, Adel El-Sokkary MM, Shata A (2020) The protective effect of Lactobacillus versus 5-aminosalicylic acid in ulcerative colitis model by modulation of gut microbiota and Nrf2/Ho-1 pathway. Life Sci 256:117927. https://doi.org/10.1016/j.lfs.2020.117927

El-Baz AM, Shata A, Hassan HM, El-Sokkary MMA, Khodir AE (2021) The therapeutic role of lactobacillus and montelukast in combination with metformin in diabetes mellitus complications through modulation of gut microbiota and suppression of oxidative stress. Int Immunopharmacol 96:107757. https://doi.org/10.1016/j.intimp.2021.107757

El-Baz AM, El-Ganiny AM, Hellal D, Anwer HM, El-Aziz HAA, Tharwat IE, El-Adawy MA, Helal SEM, Mohamed MTA, Azb TM, Elshafaey HM, Shalata AA, Elmeligi SM, Abdelbary NH, El-Kott AF, Al-Saeed FA, Salem ET, El-Sokkary MMA, Shata A, Shabaan AA (2023) Valuable effects of lactobacillus and citicoline on steatohepatitis: role of Nrf2/HO-1 and gut microbiota. AMB Express 13(1):57. https://doi.org/10.1186/s13568-023-01561-8

El-Derany MO, El-Demerdash E (2020) Pyrvinium pamoate attenuates non-alcoholic steatohepatitis: insight on hedgehog/Gli and Wnt/β-catenin signaling crosstalk. Biochem Pharmacol 177:113942. https://doi.org/10.1016/j.bcp.2020.113942

Essam RM, Ahmed LA, Abdelsalam RM, El-Khatib AS (2019) Phosphodiesterase-1 and 4 inhibitors ameliorate liver fibrosis in rats: modulation of cAMP/CREB/TLR4 inflammatory and fibrogenic pathways. Life Sci 222:245–254. https://doi.org/10.1016/j.lfs.2019.03.014

Fooladi AAI, Yazdi MH, Pourmand MR, Mirshafiey A, Hassan ZM, Azizi T, Mahdavi M, Dallal MMS (2015) Th1 cytokine production induced by *Lactobacillus acidophilus* in BALB/c mice bearing transplanted breast tumor. Jundishapur J Microbiol 8(4):e17354

Forny-Germano L, De Felice FG, Vieira M (2018) The role of leptin and adiponectin in obesity-associated cognitive decline and Alzheimer's disease. Front Neurosci 12:1027. https://doi.org/10.3389/fnins.2018.01027

Fossati P, Prencipe L (1982) Serum triglycerides determined colorimetrically with an enzyme that produces hydrogen peroxide. Clin Chem 28(10):2077–2080

Galicia-Moreno M, Lucano-Landeros S, Monroy-Ramirez HC, Silva-Gomez J, Gutierrez-Cuevas J, Santos A, Armendariz-Borunda J (2020) Roles of Nrf2 in Liver diseases: molecular, pharmacological, and epigenetic aspects. Antioxid (Basel Switzerland) 9(10):980 https://doi.org/10.3390/antiox9100980

Garcia-Castillo V, Komatsu R, Clua P, Indo Y, Takagi M, Salva S, Islam MA, Alvarez S, Takahashi H, Garcia-Cancino A (2019) Evaluation of the immunomodulatory activities of the probiotic strain *Lactobacillus fermentum* UCO-979 C. Front Immunol 10:1376

Gérard-Monnier D, Erdelmeier I, Régnard K, Moze-Henry N, Yadan J-C, Chaudière J (1998) Reactions of 1-methyl-2-phenylindole with malondialdehyde and 4-hydroxyalkenals. Analytical applications to a colorimetric assay of lipid peroxidation. Chem Res Toxicol 11(10):1176–1183. https://doi.org/10.1021/tx9701790

Gómez-Zorita S, Aguirre L, Milton-Laskibar I, Fernández-Quintela A, Trepiana J, Kajarabille N, Mosqueda-Solís A, González M, Portillo MP (2019) Relationship between changes in microbiota and liver steatosis induced by high-fat feeding-a review of rodent models. Nutrients https://doi.org/10.3390/nu11092156

Guimaraes EL, Empsen C, Geerts A, van Grunsven LA (2010) Advanced glycation end products induce production of reactive oxygen species via the activation of NADPH oxidase in murine hepatic stellate cells. J Hepatol 52(3):389–397 https://doi.org/10.1016/j.jhep.2009.12.007

Ishak K, Baptista A, Bianchi L, Callea F, De Groote J, Gudat F, Denk H, Desmet V, Korb G, MacSween RN et al (1995) Histological grading and staging of chronic hepatitis. J Hepatol 22(6):696–699. https://doi.org/10.1016/0168-8278(95)80226-6

Jayakumar S, Loomba R (2019) Review article: emerging role of the gut microbiome in the progression of nonalcoholic fatty liver disease and potential therapeutic implications. Aliment Pharmacol Ther 50(2):144–158. https://doi.org/10.1111/apt.15314

Khalaf EM, Hassan HM, El-Baz AM, Shata A, Khodir AE, Yousef ME, Elgharabawy RM, Nouh NA, Saleh S, Bin-Meferij MM, El-kott AF, El-Sokkary MMA, Eissa H (2022) A novel therapeutic combination of dapagliflozin, Lactobacillus and crocin attenuates diabetic cardiomyopathy in rats: role of oxidative stress, gut microbiota, and PPARγ activation. Eur J Pharmacol 931:175172. https://doi.org/10.1016/j.ejphar.2022.175172

Kim HN, Joo EJ, Cheong HS, Kim Y, Kim HL, Shin H, Chang Y, Ryu S (2019) Gut microbiota and risk of Persistent nonalcoholic fatty liver diseases. J Clin Med https://doi.org/10.3390/jcm8081089

Koopman N, Molinaro A, Nieuwdorp M, Holleboom AG (2019) Review article: can bugs be drugs? The potential of probiotics and prebiotics as treatment for non-alcoholic fatty liver disease. Aliment Pharmacol Ther 50(6):628–639. https://doi.org/10.1111/apt.15416

Lee NY, Shin MJ, Youn GS, Yoon SJ, Choi YR, Kim HS, Gupta H, Han SH, Kim BK, Lee DY, Park TS, Sung H, Kim BY, Suk KT (2021) Lactobacillus attenuates progression of nonalcoholic fatty liver disease by lowering cholesterol and steatosis. Clin Mol Hepatol 27(1):110–124. https://doi.org/10.3350/cmh.2020.0125

Li L, Chen L, Hu L, Liu Y, Sun HY, Tang J, Hou YJ, Chang YX, Tu QQ, Feng GS, Shen F, Wu MC, Wang HY (2011) Nuclear factor high-mobility group box1 mediating the activation of toll-like receptor 4 signaling in hepatocytes in the early stage of nonalcoholic fatty liver disease in mice. Hepatology 54(5):1620–1630. https://doi.org/10.1002/hep.24552

Li X, Hong J, Wang Y, Pei M, Wang L, Gong Z (2021) Trimethylamine-N-Oxide pathway: a potential target for the treatment of MAFLD. Front Mol Biosci 8:733507. https://doi.org/10.3389/fmolb.2021.733507

Liu L, Geng Y, Xiong C (2023) Impact of Porphyromonas gingivalis-odontogenic infection on the pathogenesis of non-alcoholic fatty liver disease. Ann Med 55(2):2255825. https://doi.org/10.1080/07853890.2023.2255825

Lonardo A, Nascimbeni F, Mantovani A, Targher G (2018) Hypertension, diabetes, atherosclerosis and NASH: cause or consequence? J Hepatol 68(2):335–352. https://doi.org/10.1016/j.jhep.2017.09.021

Lopes-Virella MF, Stone P, Ellis S, Colwell JA (1977) Cholesterol determination in high-density lipoproteins separated by three different methods. Clin Chem 23(5):882–884

Mantovani A, Dalbeni A (2021) Treatments for NAFLD: state of art. Int J Mol Sci 22(5):2350. https://doi.org/10.3390/ijms22052350

Mardinoglu A, Shoaie S, Bergentall M, Ghaffari P, Zhang C, Larsson E, Bäckhed F, Nielsen J (2015) The gut microbiota modulates host amino acid and glutathione metabolism in mice. Mol Syst Biol 11(10):834. https://doi.org/10.15252/msb.20156487

Marklund S, Marklund G (1974) Involvement of the superoxide anion radical in the autoxidation of pyrogallol and a convenient assay for superoxide dismutase. Eur J Biochem 47(3):469–474. https://doi.org/10.1111/j.1432-1033.1974.tb03714.x

Mazzotti A, Caletti MT, Sasdelli AS, Brodosi L, Marchesini GJDD (2016) Pathophysiology of nonalcoholic fatty liver disease: lifestyle-gut-gene interaction. Dig Dis 34(Suppl 1):3–10

Mijangos-Trejo A, Nuño-Lambarri N, Barbero-Becerra V, Uribe-Esquivel M, Vidal-Cevallos P, Chávez-Tapia N (2023) Prebiotics and Probiotics: therapeutic tools for nonalcoholic fatty liver disease. Int J Mol Sci https://doi.org/10.3390/ijms241914918

Miranda KM, Espey MG, Wink DA (2001) A rapid, simple spectrophotometric method for simultaneous detection of nitrate and nitrite. Nitric Oxide 5(1):62–71. https://doi.org/10.1006/niox.2000.0319

Moron MS, Depierre JW, Mannervik B (1979) Levels of glutathione, glutathione reductase and glutathione S-transferase activities in rat lung and liver. Biochimica et Biophysica Acta (BBA) - Gen Subj 582(1):67–78. https://doi.org/10.1016/0304-4165(79)90289-7

Petric Z, Paixão P, Filipe A, Guimarães Morais J (2023) Clinical pharmacology of Vinpocetine: Properties Revisited and introduction of a Population Pharmacokinetic Model for its Metabolite, Apovincaminic Acid (AVA). Pharmaceutics https://doi.org/10.3390/pharmaceutics15102502

Postic C, Girard J (2008) Contribution of de novo fatty acid synthesis to hepatic steatosis and insulin resistance: lessons from genetically engineered mice. J Clin Invest 118(3):829–838. https://doi.org/10.1172/JCI34275

Rom O, Liu Y, Liu Z, Zhao Y, Wu J, Ghrayeb A, Villacorta L, Fan Y, Chang L, Wang L, Liu C, Yang D, Song J, Rech JC, Guo Y, Wang H, Zhao G, Liang W, Koike Y, Lu H, Koike T, Hayek T, Pennathur S, Xi C, Wen B, Sun D, Garcia-Barrio MT, Aviram

M, Gottlieb E, Mor I, Liu W, Zhang J, Chen YE (2020) Glycine-based treatment ameliorates NAFLD by modulating fatty acid oxidation, glutathione synthesis, and the gut microbiome. Sci Transl Med https://doi.org/10.1126/scitranslmed.aaz2841

Saeedi BJ, Liu KH, Owens JA, Hunter-Chang S, Camacho MC, Eboka RU, Chandrasekharan B, Baker NF, Darby TM, Robinson BS, Jones RM, Jones DP, Neish AS (2020) Gut-resident Lactobacilli activate hepatic Nrf2 and protect against oxidative liver injury. Cell Metabol 31(5):956–968e5. https://doi.org/10.1016/j.cmet.2020.03.006

Saltzman ET, Palacios T, Thomsen M, Vitetta L (2018) Intestinal microbiome shifts, dysbiosis, inflammation, and non-alcoholic fatty liver disease. Front Microbiol 9:61

Shaker ME (2022) The contribution of sterile inflammation to the fatty liver disease and the potential therapies. Biomed Pharmacother 148:112789. https://doi.org/10.1016/j.biopha.2022.112789

Shen F, Zheng R-D, Sun X-Q, Ding W-J, Wang X-Y, Fan J-G (2017) Gut microbiota dysbiosis in patients with non-alcoholic fatty liver disease. Hepatobiliary Pancreat Dis Int 16(4):375–381

Sims GP, Rowe DC, Rietdijk ST, Herbst R, Coyle AJ (2010) HMGB1 and RAGE in inflammation and cancer. Annu Rev Immunol 28:367–388. https://doi.org/10.1146/annurev.immunol.021908.132603

Solano-Urrusquieta A, Morales-González JA, Castro-Narro GE, Cerda-Reyes E, Flores-Rangel PD, Fierros-Oceguera R (2020) NRF-2 and nonalcoholic fatty liver disease. Ann Hepatol 19(5):458–465. https://doi.org/10.1016/j.aohep.2019.11.010

Su X, Chen S, Liu J, Feng Y, Han E, Hao X, Liao M, Cai J, Zhang S, Niu J, He S, Huang S, Lo K, Zeng F (2024) Composition of gut microbiota and non-alcoholic fatty liver disease: a systematic review and meta-analysis. Obes Reviews: Official J Int Association Study Obes 25(1):e13646. https://doi.org/10.1111/obr.13646

Wahlang B, McClain C, Barve S, Gobejishvili L (2018) Role of cAMP and phosphodiesterase signaling in liver health and disease. Cell Signal 49:105–115. https://doi.org/10.1016/j.cellsig.2018.06.005

Wang B, Jiang X, Cao M, Ge J, Bao Q, Tang L, Chen Y, Li L (2016) Altered fecal microbiota correlates with liver biochemistry in nonobese patients with non-alcoholic fatty liver disease. Sci Rep 6:32002. https://doi.org/10.1038/srep32002

Wong SH, Kwong TN, Chow T-C, Luk AK, Dai RZ, Nakatsu G, Lam TY, Zhang L, Wu JC, Chan FK (2017) Quantitation of faecal Fusobacterium improves faecal immunochemical test in detecting advanced colorectal neoplasia. Gut 66(8):1441–1448

Yan L, Li Y, Tan T, Qi J, Fang J, Guo H, Ren Z, Gou L, Geng Y, Cui H, Shen L, Yu S, Wang Z, Zuo Z (2023) RAGE-TLR4 crosstalk is the key mechanism by which high glucose enhances the Lipopolysaccharide-Induced Inflammatory response in primary bovine alveolar macrophages. Int J Mol Sci https://doi.org/10.3390/ijms24087007

Yilmaz Y (2012) Review article: is non-alcoholic fatty liver disease a spectrum, or are steatosis and non-alcoholic steatohepatitis distinct conditions? Aliment Pharmacol Ther 36(9):815–823. https://doi.org/10.1111/apt.12046

Younossi ZM, Henry L, Bush H, Mishra A (2018) Clinical and economic burden of nonalcoholic fatty liver disease and nonalcoholic steatohepatitis. Clin Liver Dis 22(1):1–10. https://doi.org/10.1016/j.cld.2017.08.001

Zeng S, Feirt N, Goldstein M, Guarrera J, Ippagunta N, Ekong U, Dun H, Lu Y, Qu W, Schmidt AM, Emond JC (2004) Blockade of receptor for advanced glycation end product (RAGE) attenuates ischemia and reperfusion injury to the liver in mice. Hepatology 39(2):422–432. https://doi.org/10.1002/hep.20045

Zhang YS, Li JD, Yan C (2018) An update on vinpocetine: new discoveries and clinical implications. Eur J Pharmacol 819:30–34. https://doi.org/10.1016/j.ejphar.2017.11.041

Zhao YY, Yu JZ, Li QY, Ma CG, Lu CZ, Xiao BG (2011) TSPO-specific ligand vinpocetine exerts a neuroprotective effect by suppressing microglial inflammation. Neuron Glia Biol 7(2–4):187–197. https://doi.org/10.1017/S1740925X12000129

Zhong H, Li X, Zhou S, Jiang P, Liu X, Ouyang M, Nie Y, Chen X, Zhang L, Liu Y, Tao T, Tang J (2020) Interplay between RAGE and TLR4 regulates HMGB1-induced inflammation by promoting cell surface expression of RAGE and TLR4. J Immunol 205(3):767–775 https://doi.org/10.4049/jimmunol.1900860

Publisher's Note